Available online at www.sciencedirect.com
ScienceDirect
Micron 40 (2009) 74–79
micron
www.elsevier.com/locate/micron

Electronic structure of Pd nanoparticles on carbon nanotubes

A. Felten [a], J. Ghijsen [a], J.-J. Pireaux [a], W. Drube [b], R.L. Johnson [c], D. Liang [d], M. Hecq [e], G. Van Tendeloo [d], C. Bittencourt [e,*]

[a] *LISE, FUNDP—University of Namur, B-5000 Namur, Belgium*
[b] *HASYLAB, DESY, D-22603 Hamburg, Germany*
[c] *Institut für Experimentalphysik, Hamburg University, D-22761 Hamburg, Germany*
[d] *EMAT, University of Antwerp, B-2020 Antwerp, Belgium*
[e] *LCIA, University of Mons-Hainaut, Avenue Nicolas Copernic 1, B-7000 Mons, Belgium*

Received 12 October 2007; received in revised form 10 December 2007; accepted 25 January 2008

Abstract

The effect of the oxygen plasma treatment on the electronic states of multi-wall carbon nanotubes (MWCNTs) is analyzed by X-ray photoemission measurements (XPS) and UPS, both using synchrotron radiation. It is found that the plasma treatment effectively grafts oxygen at the CNT-surface. Thereafter, the interaction between evaporated Pd and pristine or oxygen plasma-treated MWCNTs is investigated. Pd is found to nucleate at defective sites, whether initially present or introduced by oxygen plasma treatment. The plasma treatment induced a uniform dispersion of Pd clusters at the CNT-surface. The absence of additional features in the Pd 3d and C 1s core levels spectra testifies that no Pd–C bond is formed. The shift of the Pd 3d core level towards high-binding energy for the smallest clusters is attributed to the Coulomb energy of the charged final state.

Keywords: CNTs; Chemical functionalization; Photoelectron spectroscopy

1. Introduction

More than a decade after their first observation, CNTs are still at the center of the scientific community interest due to their unique properties; they are molecules around their circumference while they are almost infinite crystals along their axis. The well-defined tubular crystalline structure composed by rolled graphene sheets with a diameter of nanometer size and their length up to a few microns is a perfect playing ground for hosting new scientific concepts with the potential for several promising technological applications (Saito et al., 1998).

However, the non-reactive nature of the CNT-surface prevents their optimal integration in complex assemblies (Ciraci et al., 2004). Consequently, an important step for achieving true technological applications is the integration of CNTs with other materials, ranging from inorganic compounds and polymer coating to biomolecules. In order to achieve efficient integration, it is necessary to activate the CNT-surface, which shows an inherently low chemical reactivity (Kuchibhatla et al., 2007). One promising approach to tackle this problem is to tailor chemical properties of the CNT-surface by post-growth treatments such as by grafting molecules or suitable nanostructures to the sidewall of the CNTs (Bittencourt et al., 2007; Ciraci et al., 2004; Ruelle et al., 2007; Zhu and Kaxiras, 2006). Reports on the post-treatment potentiality are given by theoretical studies which predict that by grafting metal clusters at the CNTs surface their reactivity towards a specific gas increases (Ionescu et al., 2006). In addition, nanostructured materials composed by CNTs decorated with metal nanoparticles such as Pt or Ru or bimetallic Pd/Rh nanoparticles are reported to display good catalytic behavior (Larciprete et al., 2006).

Among the metals used to decorate CNTs, Pd appears to be particularly important since besides the catalytic behavior found for Pd decorated CNTs, Pd is considered the most promising metal to achieve transparent contacts; ballistic transmission of electrons was reported for the Pd–CNT contact (Javey et al., 2003). The interaction between CNTs and metal contacts and the resulting electronic structure are crucial for the performance of CNT devices (Javey et al., 2003). Experimental studies showed that the metal used as an electrode and the variation in nanotube diameter are the two main parameters

* Corresponding author.
E-mail address: carla.bittencourt@materianova.be (C. Bittencourt).

0968-4328/$ – see front matter
doi:10.1016/j.micron.2008.01.013

responsible for the performance of CNFET (Chen et al., 2005), with the best performance achieved by combining Pd contacts with CNTs of diameter larger than 1.4 nm. In these experimental studies, the details of the interface geometry are believed to affect the nature of the contact.

The understanding of the interaction between Pd atoms and CNT-surface is a key issue in the design and optimization of practical applications. In the present study of the Pd–CNT interaction, pristine and oxygen plasma-treated multi-wall carbon nanotubes (MWCNTs) with different amounts of Pd evaporated onto their surface were analyzed by high-resolution transmission electron microscopy (HRTEM) and photoemission spectroscopy (PES) techniques.

2. Experimental

X-ray photoemission measurements (XPS) were performed at beamline BW2 of HASYLAB using a photon energy of 3300 eV (Drube et al., 1995). The Au $4f_{7/2}$ peak at 84.0 eV, recorded on a reference sample was used for calibration of the binding energy scale. In order to track small photon energy drifts during the measurements, reference spectra were measured before and after each core level and valence band datasets recorded on all the samples.

The oxygen plasma treatment was performed by using inductively coupled RF-plasma (13.56 MHz) (Felten et al., 2005). After placing the CNT powder inside the plasma glow discharge, the treatment was performed at an oxygen pressure of 0.1 Torr, applying 15 W for 60 s. The samples were prepared using commercially available MWCNTs powder (www.nanocyl.com). For the photoemission analysis, the MWCNT powder was supported on a UHV-compatible conductive carbon adhesive tape. For the TEM analysis, carbon nanotubes were sonically dispersed and a drop of the solution deposited on a honeycomb carbon film supported by a copper grid. The samples were treated on their support in order to avoid dispersion inside the plasma chamber and post-treatment contaminations.

For the XPS and TEM analysis samples were prepared by depositing different amounts of Pd onto pristine and plasma-treated MWCNTs using e-beam evaporation from a high-purity Pd rod (nominally evaporated amounts of 0.3, 1.0, 2.0, 5.0, 10 and 20 Å). Sample transfer from the preparation to the XPS analysis chamber was carried out under UHV conditions, the residual pressure in the analysis chamber was 2×10^{-10} mbar. A quartz microbalance was used to calibrate the metal evaporation rate *in situ* prior to the deposition onto the CNT samples used for transmission electron microscopy and photoemission analysis. By mounting samples of pristine and plasma-treated CNTs onto the same holder, they were simultaneously exposed during the metal evaporation ensuring the same amount of Pd on each pair of samples.

High-resolution transmission electron microscopy was performed using a JEOL 3000F microscope at 300 kV.

3. Results and discussion

Fig. 1 shows the result of evaporation of 10 Å of Pd onto pristine and oxygen plasma functionalized CNTs; the formation of nanoparticles can be observed for both cases. The influence of the oxygen plasma treatment of the CNT-surface on the formation of the Pd ''overlayer'' is clear in Fig. 2 that shows high-resolution images recorded on samples prepared with different amounts of Pd (2, 5 and 10 Å) evaporated onto pristine and oxygen plasma functionalized CNTs. Compared to the evaporation on pristine CNTs (Fig. 2a–c) the nanoparticles formed at the plasma-treated CNT-surface are more uniformly dispersed (Fig. 2d–f). During the onset of the evaporation poorly dispersed nanoparticles are formed at the pristine CNT-surface (Fig. 2a). At the graphite surface, transition-metal atoms were found to be mobile and to form clusters as the cohesive energy of these metals is much larger than the adsorption enthalpy, the nucleation centers are defects (chemical or structural) at the surface (Kuhrt and Harsdorff, 1991). Considering the reported similarities between the graphite and the CNT-surfaces, it can be assumed that Pd atoms are mobile and diffuse at the CNT-surface until they find a nucleation center. Consequently, the cluster dispersion will depend on the dispersion of the defects at the CNT-surface.

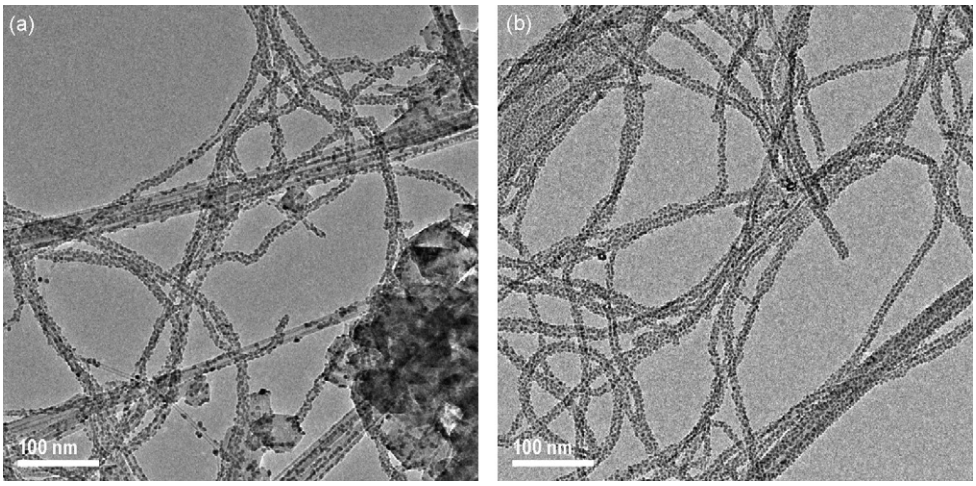

Fig. 1. HRTEM image of Pd on (a) MWCNTs and (b) oxygen plasma-treated MWCNTs. Thermal evaporation of 10 Å (nominal deposition).

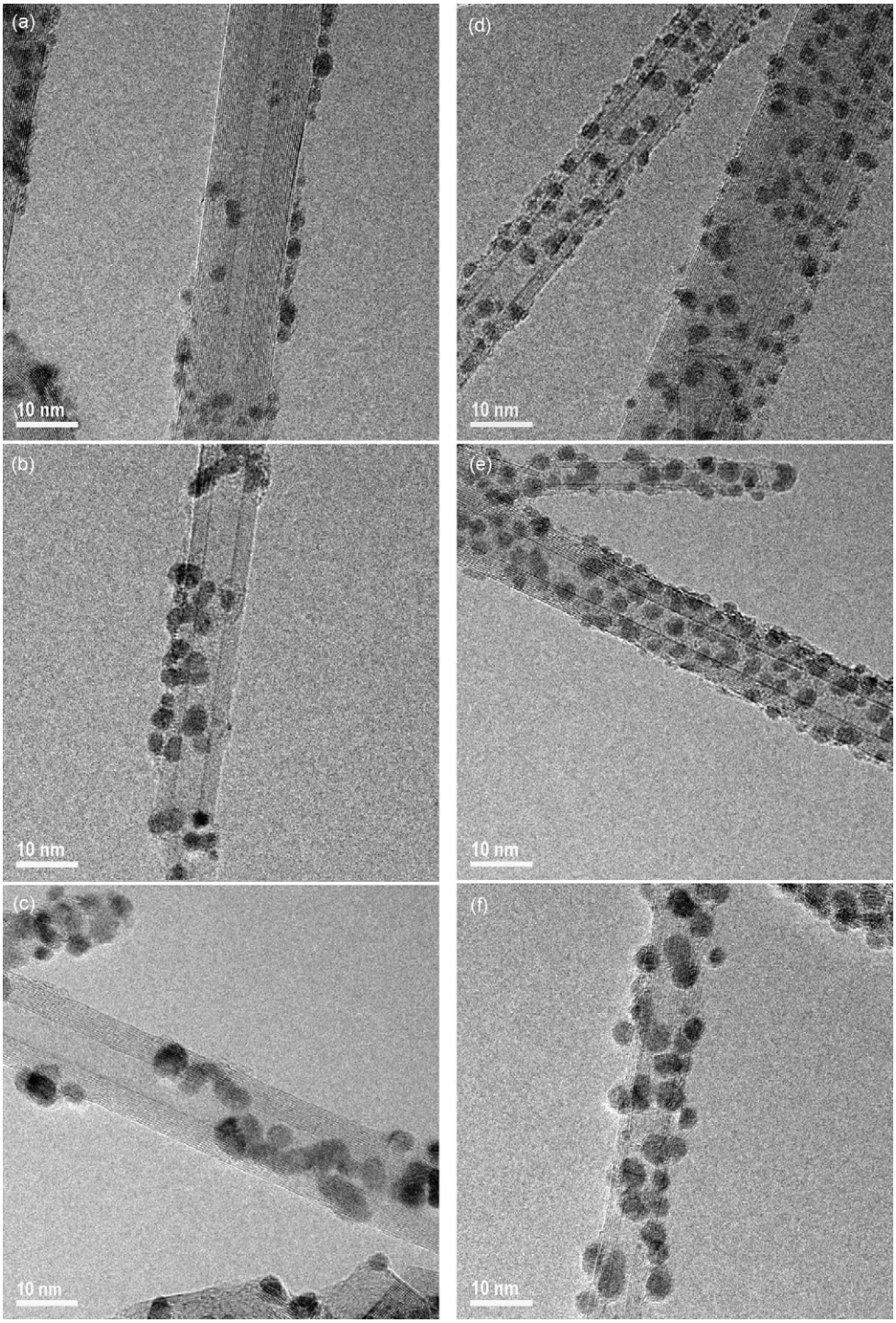

Fig. 2. HRTEM images of different thermally evaporated Pd amounts on MWCNTs (nominal deposition of (a) 2 Å, (b) 5 Å and (c) 10 Å) and on oxygen plasma-treated MWCNTs (nominal deposition of (d) 2 Å, (e) 5 Å and (f) 10 Å).

In the majority of synthesis methods, it cannot be avoided to expose CNTs to oxygen gases in air during sample preparation. Therefore, understanding the effect of exposing CNTs to oxygen is of importance for controllability and stability of CNT-based electronic devices. As will be discussed, oxygen plasma treatment grafts oxygen functional groups at the CNTs surface as a result of O_2 dissociation on vacancies created during the plasma treatment. Considering that Pd strongly interacts with oxygen atoms (Cai et al., 1998), it can be suggested that Pd nucleation centers occur in the proximity of oxygenated defects created during the treatment. Therefore, the improved Pd cluster dispersion for the plasma-treated MWCNT can be attributed to the creation of dispersed oxidized vacancies at the CNT-surface by the plasma treatment.

Fig. 3 shows a HRTEM image of Pd clusters sitting on the surface of an oxygen plasma-treated MWCNT. The preserved

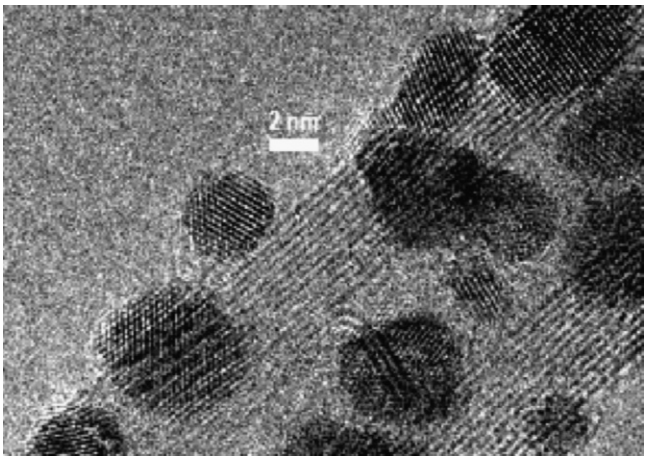

Fig. 3. HRTEM image of a Pd cluster sitting at the oxygen plasma-treated CNT-surface. Thermal evaporation of 2 Å (nominal deposition).

structural characteristics of the graphene layer under the Pd cluster suggest the absence of a Pd–C phase formation. Further indication can be obtained by XPS because it is sensitive to chemical reactions at the interface: a different chemical environment of the atoms at the interface will generally lead to the appearance of new spectral features in the XPS spectra.

Fig. 4 shows the comparison of typical C 1s spectra recorded on pristine and plasma-treated CNTs with corresponding spectra obtained for Pd decorated ones. The oxygen atomic concentration was measured to be 10%. Photoelectrons emitted from carbon atoms in the ''graphite-like'' walls generate a peak centered at 284.3 eV binding energy. The chemical modification produced by the plasma treatment gives rise to a broad structure peaking at 287.5 eV: it is attributed to photoelectrons emitted from carbon atoms belonging to hydroxyl (component centered at 286.2 eV), carbonyl (or ether) (component centered at 287.2 eV) and carboxyl (or ester) groups (component centered at 288.9 eV) (Felten et al., 2005). Therefore, the oxygen plasma treatment induces the grafting of oxygen species to the chemically inactive surface of the MWCNTs; the grafting of oxygen was reported to occur at defects created during the oxygen plasma treatment (Ionescu et al., 2006).

Reports on the formation of Pd carbide (PdC_x) showed that the photoelectrons emitted from the C 1s core level from carbon atoms participating in the Pd–C bond are observed at equal 282.0 eV binding energy (Han et al., 2004). Actually, in the spectra shown in Fig. 4, no additional features are observed at binding energies lower than the C 1s core level peak at 284.0 eV associated with photoelectrons emitted from the CNT-walls vicinity. Thus, the preserved structural characteristic of the graphene layer underneath the Pd cluster combined with the absence of additional C 1s features in the XPS spectra testify the absence of a mixed Pd–C phase at the cluster–CNT interface.

This conclusion is further corroborated by core-level spectroscopy of the Pd 3d doublet. The evolution of the Pd 3d lines for a sequence of Pd evaporations onto pristine MWCNTs is shown in Fig. 5. No additional features accompanying the Pd 3d doublet are observed, however, the Pd 3d peaks shift towards higher binding energy for decreasing evaporated amounts of Pd.

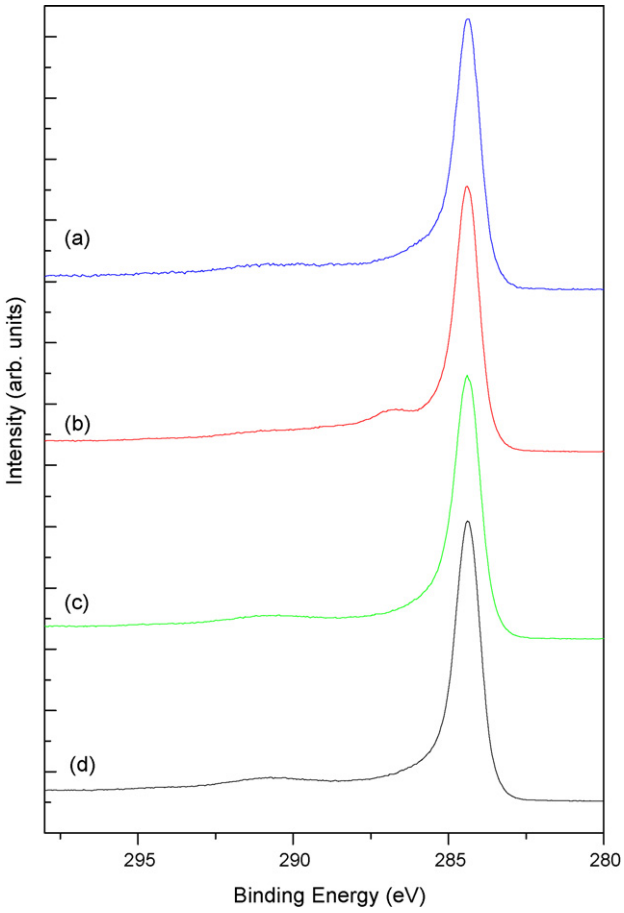

Fig. 4. C 1s core level spectra ($h\nu = 3300$ eV) recorded on (a) Pd on plasma-treated MWCNTs (nominal Pd deposition onto the CNTs surface 5 Å), (b) oxygen plasma-treated MWCNTs, (c) Pd on pristine MWCNTs and (d) pristine MWCNTs.

For supported Pd clusters this decrease in kinetic energy was reported to be mainly a consequence of a temporal charging of the nanoparticle due to the photoionization process, *i.e.*, the core level shift caused by the Coulomb energy of the charged final state (Wertheim et al., 1986).

A similar trend was observed for the clusters on oxygen plasma-treated CNTs, however, in this case for the spectra recorded on the onset of the evaporation (lower spectra, Fig. 4) the Pd 3d line exhibits an increased intensity at higher binding energies. This does not, however, reflect the formation of a Pd–C bond, rather this chemically shifted component can be identified as PdO (as no corresponding feature was observed in the C 1s lines). For increasing evaporation amounts of Pd the relative intensity of Pd 3d associated to Pd^0 increases, suggesting that the Pd–O bond exists near the interface between the Pd clusters and the CNT-surface, *i.e.*, for some clusters the interface is better described by PdO–CNT. As suggested before, the Pd nucleation centers are oxygenated vacancies created during the plasma. The decrease of the relative intensity of the component (centered at 287.5 eV) that was associated to the grafting of oxygen functions at the CNT-surface (Fig. 4) will support this assertion. Pd nanoparticles at the CNT-surface will reduce the number of photoelectrons emitted from the C 1s levels contributing for the

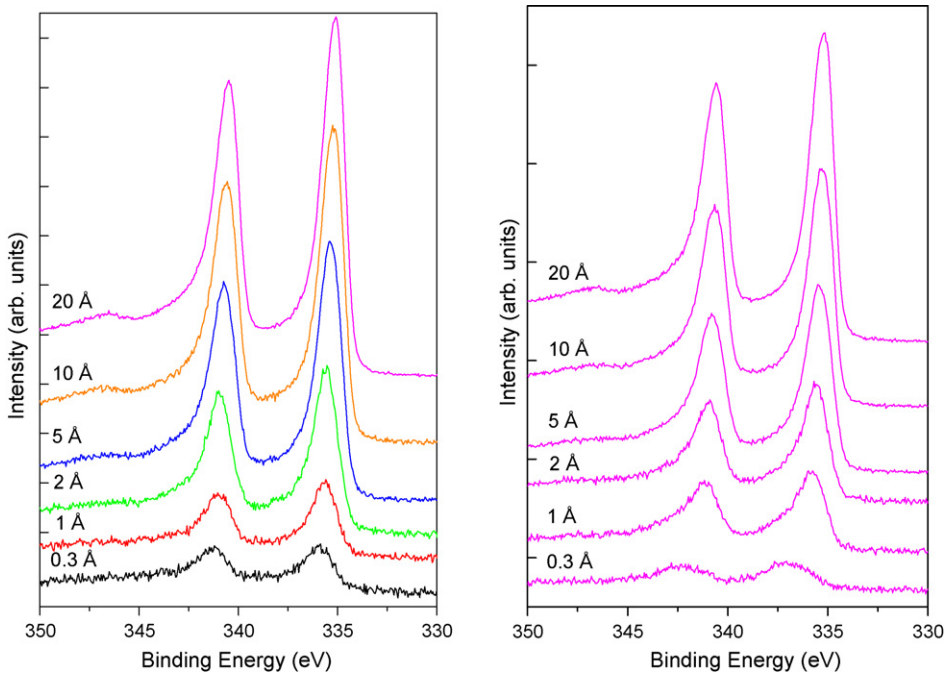

Fig. 5. $3d_{5/2}$ core level spectra ($h\nu$ = 3300 eV) recorded on (a) Pd/MWCNTs and (b) on Pd decorated oxygen plasma-treated MWCNTs. Nominal Pd deposition onto the CNT-surface: from bottom to top 0.3, 1.0, 2.0, 5.0, 10 and 20 Å.

XPS spectrum. Due to inelastic attenuation some photoelectrons emitted from carbon atoms below Pd clusters will lose part of their kinetic energy when passing through them (for increasing evaporated amounts of Pd the probability of attenuation will increase), no longer contributing to the C 1s peak. Considering that Pd nucleation centers occur mainly in the proximity of oxygenated defects, particles forming will first cover this region. Consequently, in the onset of the evaporation a pronounced reduction in the contribution of photoelectrons emitted from C atoms belonging to oxygen groups that are localized mainly under the cluster will show in the XPS spectrum.

The 3d line from Pd^0 shifts towards higher binding energy for decreasing cluster size (*i.e.*, for decreasing evaporated Pd amounts), however the energy shift magnitude cannot be compared with the one found for clusters at the pristine CNT-surface as the presence of more nucleation sites created by the plasma treatment will lead to smaller clusters (for the same amount of metal evaporated).

In the Pd valence band, the 4d density of states has a sharp peak just below E_F; consequently, fitting the Fermi cut-off in the valence band requires an explicit representation of the density of states even for the bulk metal. In addition, the drastic effect of the finite cluster size on the electronic structure makes the determination of the density of states near E_F difficult as it should be performed for each cluster size (Wertheim et al., 1986). Therefore, it is preferred in this work to monitor the valence band by tracking the centroid of the 4d band.

Fig. 6 presents the evolution of the valence band states for increasing amounts of Pd evaporated (from 0.3 to 20 Å) on pristine MWCNTs. The Pd valence band is mainly formed by 4d states partially hybridized with 5s orbitals (Wertheim et al., 1986). The level of hybridization between the initially empty

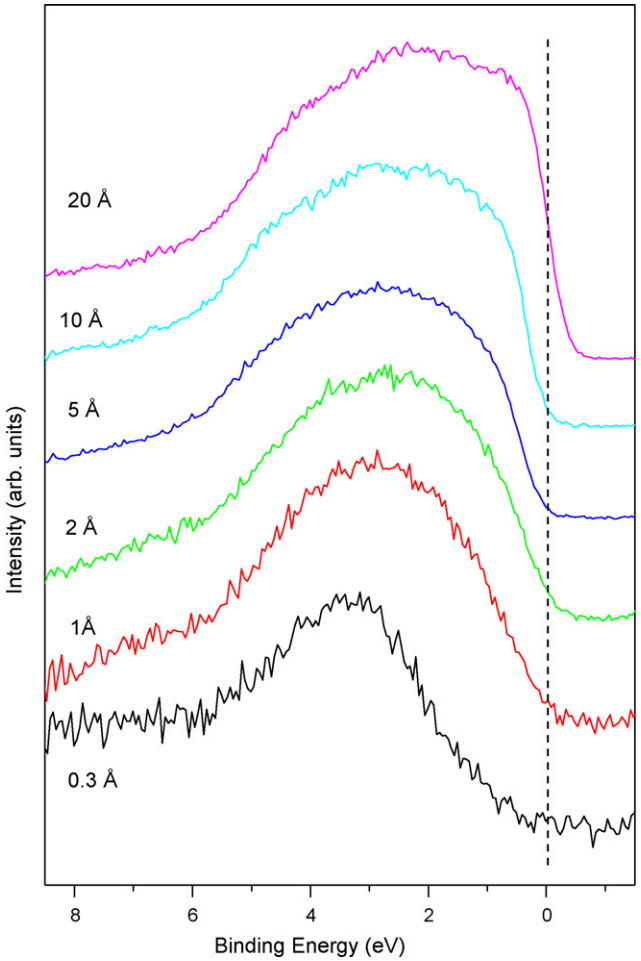

Fig. 6. Valence band spectra ($h\nu$ = 3300 eV) of Pd/MWCNTs (nominal Pd deposition onto the CNTs surface 0.3, 1.0, 2.0, 5.0, 10 and 20 Å).

$5s^0$ and the filled metal d states increases with cluster size as the d character evolves from the d^{10} configuration of the isolated atom to a more band-like configuration. Thus, the electronic structure near the Fermi level is significantly affected by the metal cluster size in the early stage of metal deposition. For increasing amounts of Pd evaporated, it can be observed the broadening of the 4d band and the shift of the centroid from 3.5 to 2.1 eV. The broadening reflects the number of Pd nearest neighbors surrounding a Pd atom and consequently the strength of the Pd–Pd interactions. Thus, the observed increase in the broadening is expected in the case of nanoparticles where the coordination number of Pd–Pd nearest neighbor increases.

As reported, the initial-state band structure changes cannot account for the positive core-electron binding energy shift observed in Pd clusters; rather, this is interpreted as a final-state effect (Wertheim et al., 1986). From Fig. 6 it is seen that the Fermi energy level of the clusters moves away from that of the substrate, shifting towards larger binding energy with decreasing cluster size. This is easily understood if one assumes the emitted photoelectron is not quickly replaced, so that the cluster is left behind with a net positive charge in the photoemission final state (Wertheim et al., 1986). The final-state energy is then increased by the Coulomb energy, which for a charged conducting sphere is $e^2/2r$. Since this final-state charge occurs whenever a photoelectron is emitted, the entire spectrum, core levels as well as the Fermi edge, appears shifted to higher binding energy.

4. Summary

The evolution of the valence band states and core-electron levels linked to the nanoclusters size was studied by XPS. The absence of additional features in the C 1s and in the Pd core level spectra testifies the absence of chemical reaction at the Pd cluster–CNT interface. Plasma treatment of CNTs in a RF-plasma of oxygen grafts oxygen to the CNT-surface that will act as an active center for Pd cluster formation inducing changes in size and dispersion of clusters evaporated onto the CNT-surface.

Acknowledgements

This work is financially supported by the Belgian Program on Interuniversity Attraction Pole (PAI 608), by DESY and the European Commission under contract RII3-CT 2004-506008 (IASFS), and by the EC under the Nano2hybrids Project (STREP, 033311). JG is a research associate of NFSR (Belgium).

References

Bittencourt, C., Felten, A., Ghijsen, J., Pireaux, J.J., Drube, W., Erni, R., Van Tendeloo, G., 2007. Decorating carbon nanotubes with nickel nanoparticles. Chem. Phys. Lett. 436, 368–372.

Cai, Y.Q., Bradshaw, A.M., Guo, Q., Goodman, D.W., 1998. The size dependence of the electronic structure of Pd clusters supported on Al_2O_3/Re(0 0 0 1). Surf. Sci. 399, L357–L363.

Chen, Z., Appenzeller, J., Knoch, J., Lin, Y.-M., Avouris, Ph., 2005. The role of metal–nanotube contact in the performance of carbon nanotube field-effect transistors. Nanoletters 5, 1497–1502.

Ciraci, S., Dag, S., Yildirim, T., Gülseren, O., Senger, R.T., 2004. Functionalized carbon nanotubes and device applications. J. Phys.: Condens. Matter 16, R901–R960.

Drube, W., Schulte-Schrepping, H., Schmidt, H.-G., Treusch, R., Materlik, G., 1995. Design and performance of the high-flux high-brightness X-ray wiggler beamline BW2 at Hasylab. Rev. Sci. Instrum. 66, 1668–1670.

Felten, A., Bittencourt, C., Pireaux, J.-J., Van Lier, G., Charlier, J.C., 2005. Radio-frequency plasma functionalization of carbon nanotubes surface O_2^-, NH_3, and CF_4 treatments. J. Appl. Phys. 98, 074308.

Han, Y.-F., Kumar, D., Sivadinarayana, C., Clearfield, A., Goodman, D.W., 2004. The formation of PdC_x over Pd-based catalysts in vapor-phase vinyl acetate synthesis: does a Pd–Au alloy catalyst resist carbide formation? Catal. Lett. 94, 131–134.

Ionescu, R., Espinosa, E.H., Sotter, E., Llobet, E., Vilanova, X., Correig, X., Felten, A., Bittencourt, C., Van Lier, G., Charlier, J.C., Pireaux, J.J., 2006. Sens. Actuator B: Chem. 113, 36–46.

Javey, A., Guo, J., Wang, Q., Lundstrom, M., Dai, H., 2003. Ballistic carbon nanotube field-effect transistors. Nature 424, 654–657.

Kuchibhatla, S.V.N.T., Karakoti, A.S., Debasis, B., Seal, S., 2007. One dimensional nanostructured materials. Progr. Mater. Sci. 52, 699–913.

Kuhrt, Ch., Harsdorff, M., 1991. Photoemission and electron microscopy of small supported palladium clusters. Surf. Sci. 245, 173–179.

Larciprete, R., Lizzit, S., Petaccia, L., Goldoni, A., 2006. NO_2 decomposition on Rh clusters supported on single-walled carbon nanotubes. Appl. Phys. Lett. 88, 243111.

Ruelle, B., Peeterbroeck, S., Gouttebaron, R., Godfroid, T., Monteverde, F., Dauchot, J.P., Alexandre, M., Hecq, M., Dubois, Ph., 2007. Functionalization of carbon nanotubes by atomic nitrogen formed in a microwave plasma Ar + N_2 and subsequent poly(ε-caprolactone) grafting. J. Mater. Chem. 17, 157–159.

Saito, R., Dresselhaus, G., Dresselhaus, M.S., 1998. Physical Properties of Carbon Nanotubes. World Scientific Publishing, Singapore.

Wertheim, G.K., DiCenzo, S.B., Buchanan, D.N.E., 1986. Noble- and transition-metal clusters: the d bands of silver and palladium. Phys. Rev. B 33, 5384–5390.

Zhu, W., Kaxiras, E., 2006. Electronic structure of Pd-covered (10,0) carbon nanotube. Phys. Status Solidi 243, 2164–2169.